EUROPEAN ORGANIZATION FOR NUCLEAR RESEARCH

CERN-EP/98-081
May 29, 1998

Silicon detectors for neutrino oscillation experiments

Eduardo do Couto e Silva[1]
CERN-EP Division,
CH 1211, Geneva, Switzerland.
(on behalf of NOMAD and TOSCA collaborations)

Abstract

This note describes the technique of using a target equipped with high resolution silicon microstrip detectors for the detection of the topological signature of decays in neutrino oscillation experiments. Two detectors are presented.

The first detector is installed in the NOMAD spectrometer at the CERN SPS neutrino beam. The target consists of four layers passive boron carbide plates (total mass of 45 kg) interleaved with five layers of silicon microstrip detectors. A total of 600 single–sided silicon microstrip detectors are used amounting to a total area of 1.14 m^2. The silicon tracker is made with the longest ladders built to date (72 cm). During the 1997 run about 8000 charged current interactions were estimated to have occurred in the target and data taking will continue in 1998. For these events it will be possible to perform a precise measurement of both vertex and kinematical variables. The second detector was installed in September 1997 in a CERN PS pion beam to investigate the possibility of combining silicon detectors and nuclear emulsions. This detector consists of 72 single–sided silicon microstrip detectors with a total surface of 0.13 m^2 distributed over four layers, providing two measurements of each of the two orthogonal coordinates. This exposure will measure the precision with which the silicon tracker can predict the position of particles in the emulsion.

Both detectors provide invaluable experience towards the construction of a large scale silicon tracker for future neutrino oscillation experiments.

Contributed paper to the
XVIII International Conference on Neutrino Physics and Astrophysics,
Takayama, Japan, June 4-9, 1998.

[1]email: Eduardo.do.Couto.e.Silva@cern.ch

1 Introduction

One of the most interesting current problems in particle physics is the possibility that neutrinos have non-vanishing masses and that there are oscillations among the different families. At present, two experiments, CHORUS and NOMAD [1, 2] are searching for the exclusive $\nu_\mu(\nu_e) \leftrightarrow \nu_\tau$ oscillation modes in the CERN-SPS beam.

Both experiments are sensitive to small mixing angles in the limit of large mass squared difference ($>$ few eV^2). Experiments with a sensitivity at least an order of magnitude larger than CHORUS and NOMAD are being actively discussed [3, 4, 5, 6, 7]. All these experiments are based on a target equipped with high resolution tracking detectors, capable of detecting the topological signature of the τ decays: either a displaced vertex or a charged track with non–zero impact parameter at the primary vertex.

To understand the design of a large surface silicon tracker for a future $\nu_\mu(\nu_e) \leftrightarrow \nu_\tau$ oscillation experiment we have built two detectors: NOMAD–STAR [8, 9], an instrumented silicon target which has been taking data in the NOMAD spectrometer since May of 1997, and a hybrid detector, which combines silicon detectors and nuclear emulsions and was installed in September 1997 in a CERN PS pion beam.

Throughout this note the NOMAD–STAR and the hybrid detectors are compared. The organization is as follows: we begin with section 2 which gives an overview of both detectors. Section 3 describes the silicon detectors. Sections 4 and 5 discuss ladder assembly and tests, respectively. In section 6 results from the mechanical survey are briefly mentioned. After that, section 7 discusses the sources of noise in a silicon detector and presents a comparison between analytical calculations and laboratory measurements. Section 8 presents a few results. Conclusions are presented in section 9.

2 Overview

Both detectors (NOMAD–STAR and hybrid), contain silicon detectors glued onto rigid structures (ladders) assembled into layers. The layers are arranged in NOMAD–STAR to provide a precise measurement of only one spatial coordinate (y). In the hybrid detector the construction permits two measurements of both x and y coordinates. Despite the larger number of readout channels in NOMAD–STAR (32000) as compared to that of the hybrid detector (15360), the readout system is identical for both, and therefore limited to one event per spill. We used the VA1 readout chip[2] which consists of 128 charge sensitive, low–power and low–noise preamplifiers followed by CR–RC shapers, track–and–hold circuitry, output multiplexing and a multiplexing calibration circuit.

[2] A commercial version of the VIKING chip [10] manufactured by IDE AS, Norway.

From the technical point of view NOMAD–STAR demonstrated that very long ladders of silicon detectors (72cm) can be read out at only one end. The hybrid detector was constructed based on the experience acquired with NOMAD–STAR. Despite its shorter ladders (18cm), as will be shown in later sections, it has a superior design.

2.1 NOMAD–STAR

The NOMAD apparatus shown schematically in Fig. 1 records the neutrino interactions produced in the active target which consists of a set of drift chambers with a fiducial mass of about 2.7 tons. Measurements of the kinematical properties of neutrino interactions produced in this target allow the identification of possible τ candidates [2]. However, the drift chamber resolution is not sufficient to provide τ identification based on topological criteria.

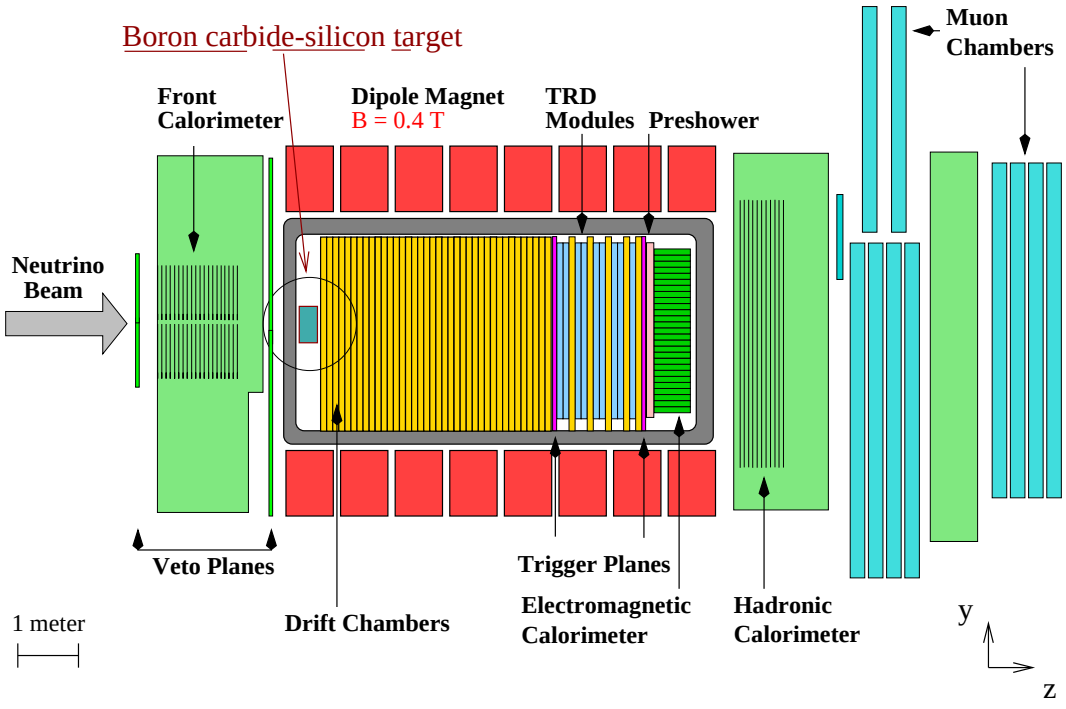

Figure 1: The NOMAD detector with the boron carbide–silicon target (NOMAD–STAR).

The target shown in Fig. 2 was installed upstream of the first NOMAD drift chamber. It consists of four layers of boron carbide (B_4C) interleaved with layers

of silicon detectors. The silicon tracker consists of 600 silicon detectors distributed over 5 layers of 10 ladders each, and covering a total active surface of 1.14 m^2.

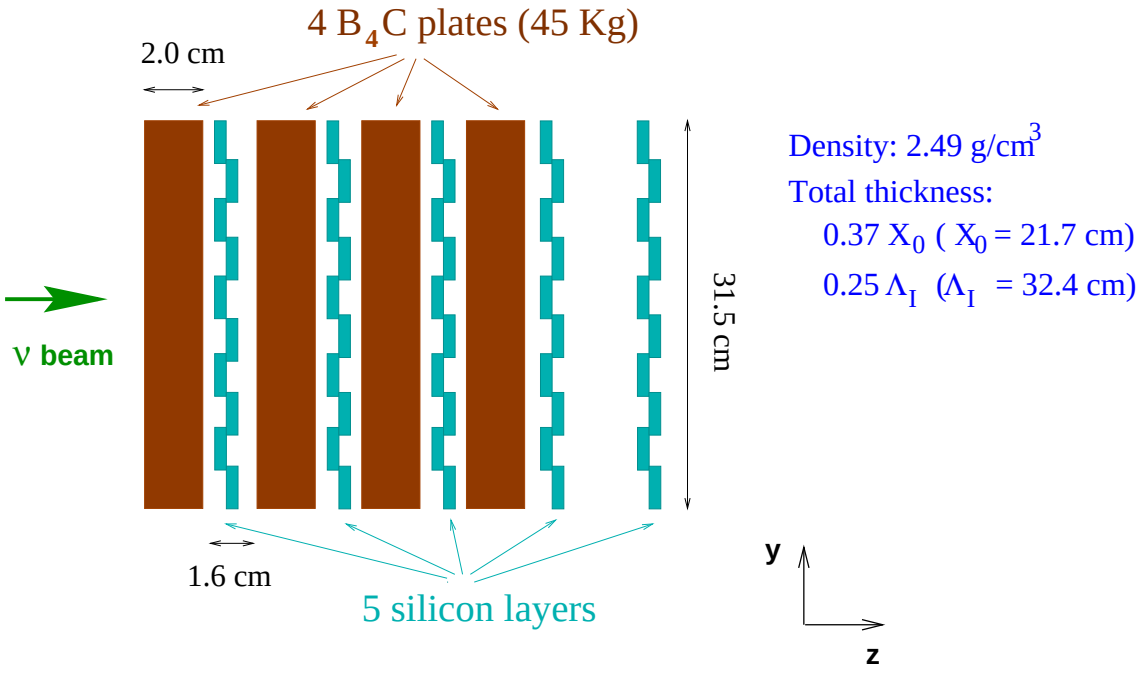

Figure 2: Schematic drawing of the side view of the silicon target.

2.2 Hybrid Detector

The hybrid detector was conceived to study how well silicon detectors can locate the position of particles in nuclear emulsion. This test was not performed in a neutrino beam but in a pion test beam.

A drawing of the set–up is shown in Fig. 3. It consists of beam counters and wire chambers placed upstream, followed by an emulsion target, a silicon tracker, an emulsion spectrometer, a honeycomb tracker and multiwire proportional chambers. A dipole magnet is used to produce a field of 0.7 Tesla.

The silicon tracker consists of 72 silicon detectors with an active surface of 0.13 m^2 distributed over 4 layers of 6 ladders each. A schematic drawing of the silicon tracker is shown in Fig. 4.

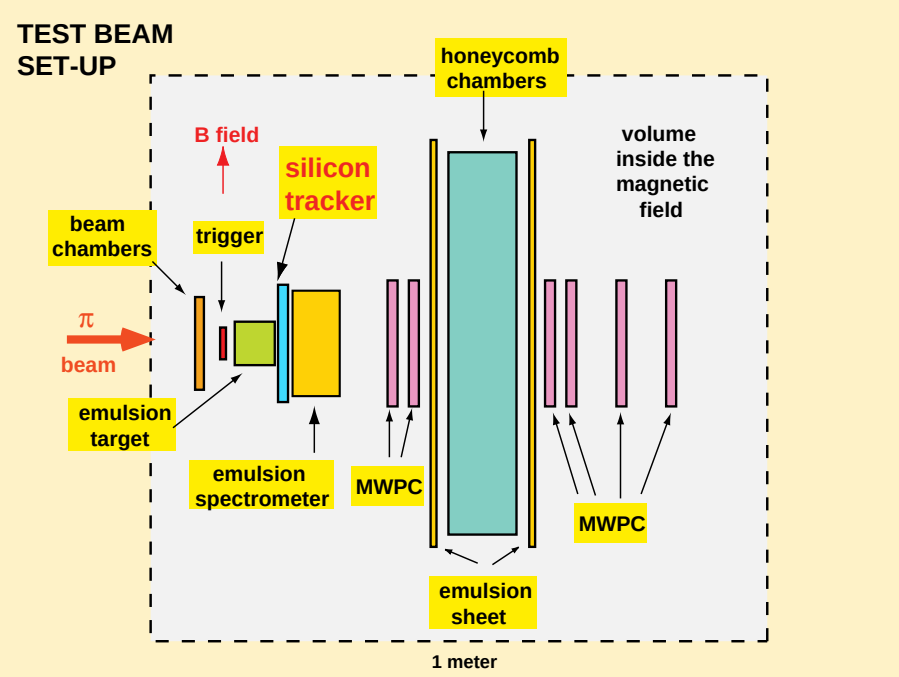

Figure 3: Schematic drawing of the test beam set–up (side view).

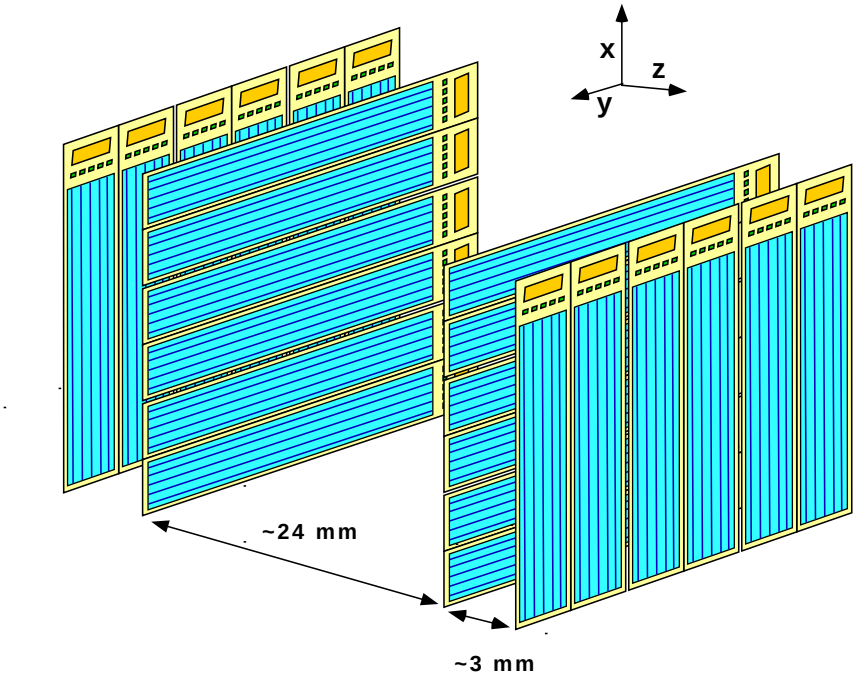

Figure 4: Schematic drawing of four silicon layers.

3 Silicon Microstrip Detectors

The silicon microstrip detectors[3] are identical to those used in the DELPHI experiment [11]. These are single–sided, 33.5 mm $\times$ 59.9 mm, with strip and readout pitches of 25 μm and 50 μm, respectively. The p^+ strips are implanted in a high resistivity 300 μm-thick n–type substrate, and are AC coupled to the electronics via a silicon oxide layer. The biasing of the strips is done via the FOXFET mechanism [12]

The testing programme has been fully described elsewhere [8]. For the ladder production it consists of visual scan of the detectors and long term leakage current measurements ($\simeq$24h) at a bias voltage of about 70 V.

3.1 NOMAD–STAR

Figure 5a shows the measured leakage current for 620 detectors.

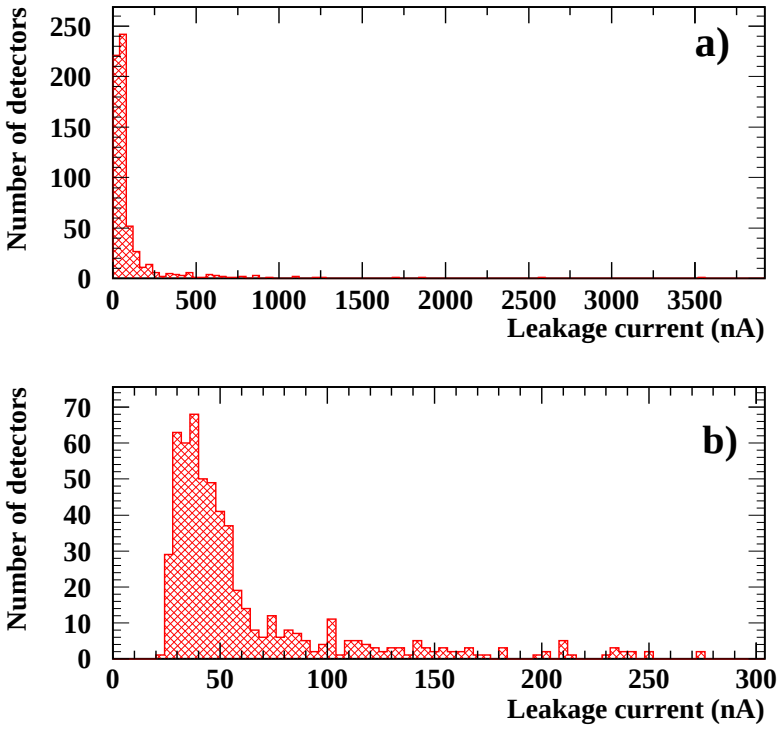

Figure 5: Leakage current for: a) all detectors: and b) only detectors with leakage current smaller than 300 nA (92% of the total).

In Fig. 5b only detectors with leakage current below 300 nA are displayed,

[3]Manufactured by Hamamatsu Photonics, Japan.

corresponding to 92% of the total number of detectors. Out of 623 detectors only 3 could not hold the bias voltage and had runaway leakage currents (> 10 μA). The detector yield of 98% reduced to 96% due to damages during and after ladder assembly.

3.2 Hybrid Detector

Figure 6a shows the measured leakage current for 100 detectors. In Fig. 6b only detectors with leakage current below 100 nA are displayed, corresponding to 92% of the total number of detectors. Only one detector had a processing error (seven interrupted floating strips) and it was therefore rejected.

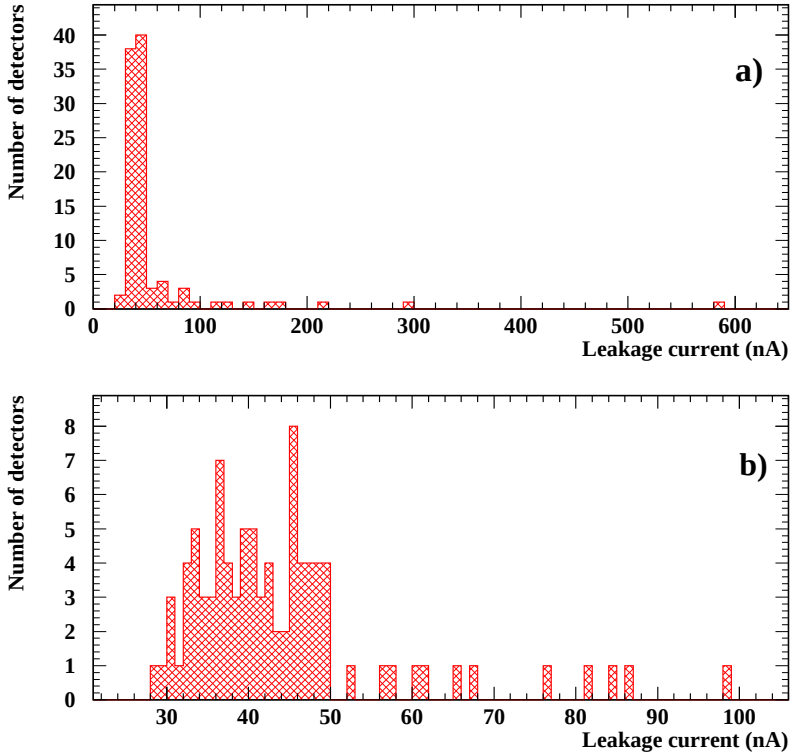

Figure 6: Leakage current distributions for: a) all detectors and b) only detectors with leakage current smaller than 100 nA (92% of the total).

We have profited from the experience acquired with NOMAD–STAR and detector yield increased to 99% with no losses during and after assembly.

4 Ladder Assembly

Detectors are glued onto a carbon fiber back bone and daisy-chained electrically using wire bonds. A thin foil of insulating material electrically isolates detectors from the carbon fiber. One of the ends of the ladder is glued to an aluminum support that carries a hybrid printed circuit board, fixing and alignment holes. The readout chips are mounted on the hybrid board. At the opposite end, a gold–plated ceramic plate serves as a ground plate. To compensate for thermal expansion the end piece at the far end of the ladder is allowed to move. The backplane of each detector is connected to the bias line in the hybrid using 10 MΩ resistors so that the leakage current for each detector can be measured separately. A capacitor connects the backplane of the last detector in each ladder. A voltage step applied to this capacitor induces charge pulses in all strips for tests and calibration (backplane pulsing).

4.1 NOMAD–STAR

Figure 7 illustrates the assembly of a ladder for NOMAD–STAR.

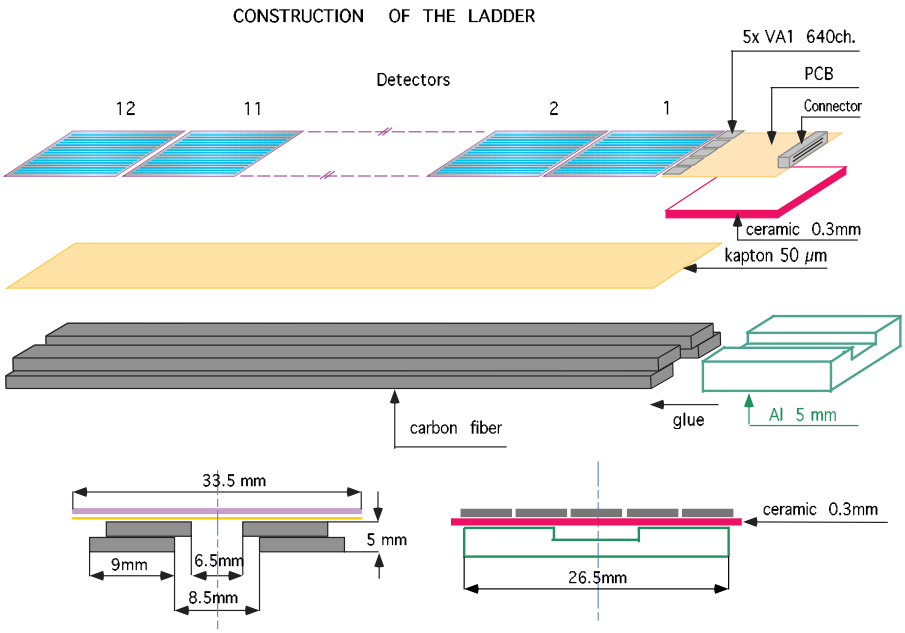

Figure 7: Schematic drawing of a ladder for NOMAD–STAR.

Twelve silicon detectors are glued onto the carbon fiber back bone which has a total thickness of 5 mm. Detectors and carbon fiber are isolated from each

other via a kapton foil.

4.2 Hybrid Detector

Figure 8 illustrates the assembly of a ladder for the silicon tracker of the hybrid detector.

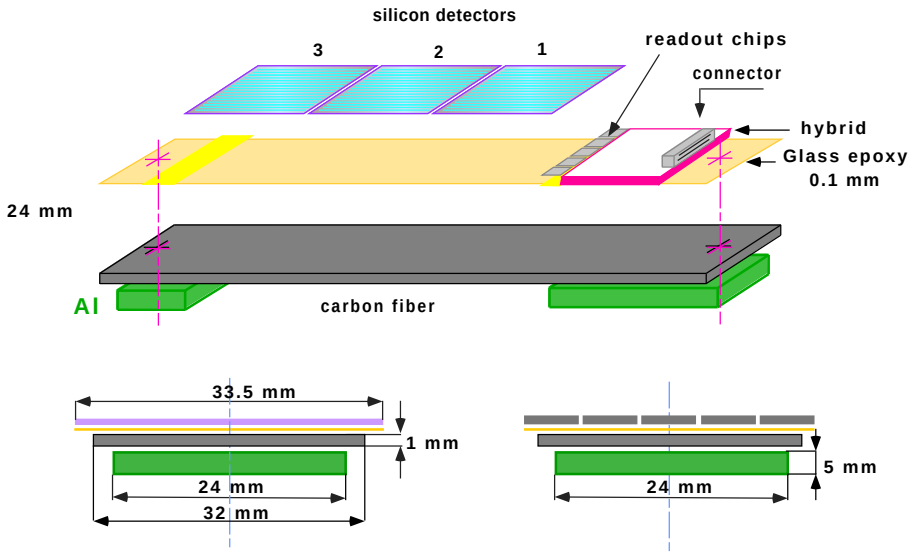

Figure 8: Schematic drawing of a ladder for the silicon tracker of the hybrid detector.

Three silicon detectors are glued onto the carbon fiber back bone which has a total thickness of 1 mm, therefore reducing the effects of multiple scattering. Detectors and carbon fiber are isolated via a glass fiber foil with a printed circuit. The printed circuit routes the lines necessary for the leakage current and backplane pulsing measurements. This new design facilitates ladder debugging and reduces the number of gluing steps during ladder assembly.

5 Ladder Tests

The testing programme for the ladders follow that of [9]: measurements of noise, leakage current and backplane pulsing. Each ladder was operated with a reverse bias voltage of 60 V with gate and drain grounded. The signal–to–noise ratio was measured using a radioactive ruthenium source[4]. The signal–to–noise ratio

[4]Electrons emitted with maximum energy of about 3.5 MeV.

is defined as the fitted peak position when a Landau distribution convolved with a Gaussian is used to fit the charge distribution due to the source.

5.1 NOMAD–STAR

The summary of the ladder tests after repair is shown in Figs. 9a and 9b. Time constraints did not permit to fully debug all ladders. As a result, a few ladders had a large number defective channels ($> 3\%$) and high leakage currents (> 3 μA). On average a ladder has a signal–to–noise ratio of 16:1, leakage current of 2 μA and 1.4% of defective channels.

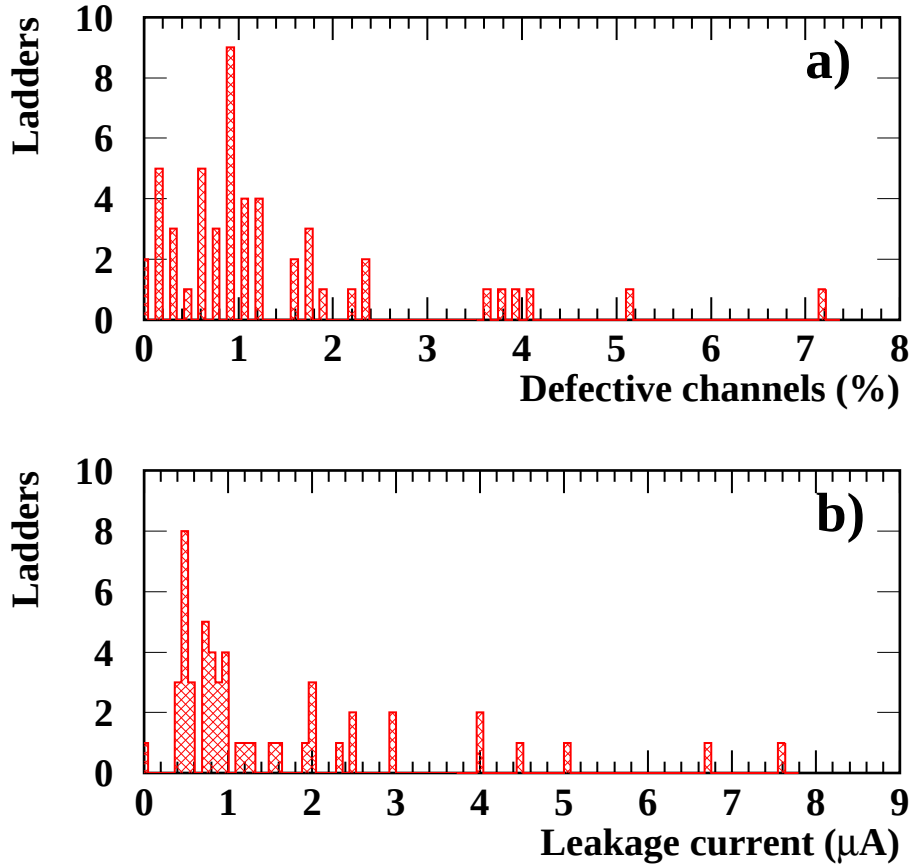

Figure 9: a) Percentage of defective channels for all ladders, b) leakage current for all ladders.

5.2 Hybrid Detector

The summary of the ladder tests after repair is presented in Figs. 10a and 10b. In average a ladder has a signal–to–noise ratio of 60:1, leakage current of 150 nA and 0.2% defective channels. Since these ladders are shorter than those of NOMAD–STAR, a lower leakage current and a higher signal–to–noise ratio are expected. Nevertheless, combining these results with those of section 7, one clearly sees the improved performance of the hybrid detector.

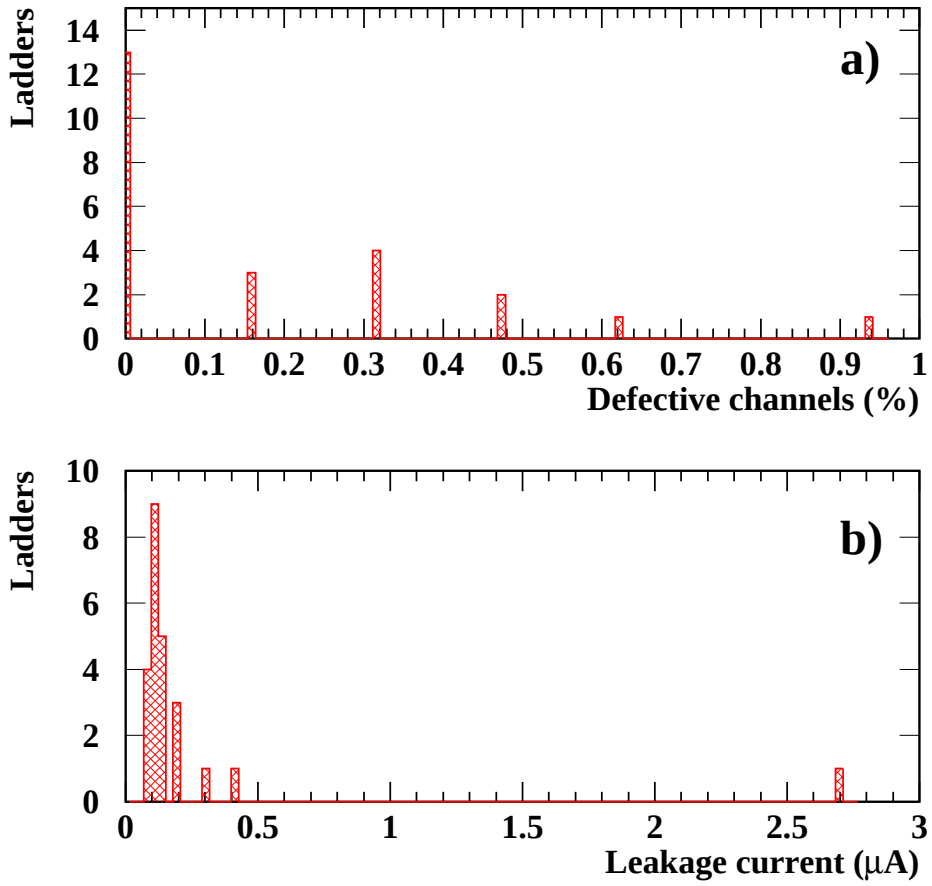

Figure 10: a) Percentage of defective channels for all ladders, b) leakage current for all ladders.

6 Ladder Survey

In order to have a position resolution of less than 10 μm, each layer had to be surveyed accurately. A description of the survey can be found elsewhere [8]. The

resolution in both X and Y were determined precise marks at the corners of each detector. The resolution for the Z–coordinate is based on the reproducibility of measurements performed by different surveyors.

6.1 NOMAD–STAR

The resolution of the surveying system was found to be $\sigma_x \sim 6$ μm and $\sigma_y \sim 7$ μm and $\sigma_z \sim 14$ μm. The systematic uncertainty in the X-, Y- and Z-positions was determined from the reproducibility of the results from different operators and on comparisons of results with the layers before and after installation in the support structure. These were: $\sigma_x \sim 6$ μm, $\sigma_y \sim 7$ μm and $\sigma_z \sim 31$ μm.

6.2 Hybrid Detector

As shown in Fig. 11 the resolutions in X and Y for the surveying system are better than 5 μm.

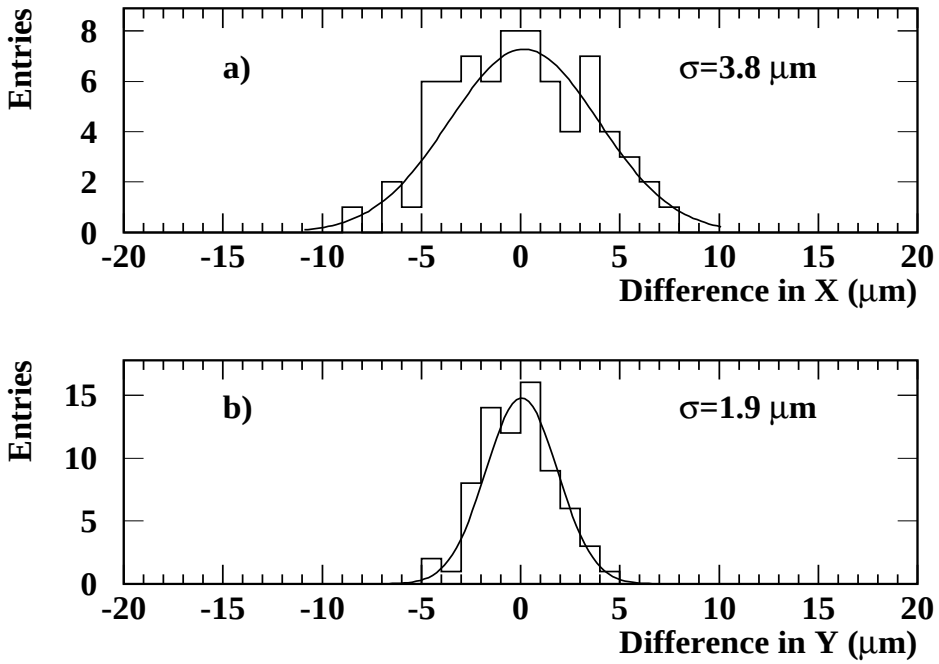

Figure 11: Resolution of the surveying system. Systematic differences in the measurements of the coordinates a) X and b) Y.

The improvement seen with respect to the results from NOMAD–STAR is due to a better calibration of the survey equipment. Due to time constraint, the requirement on the resolution for the Z coordinate was relaxed to be better than

50 μm. The systematical errors due to the mounting and dismounting of the ladders and the rotations of the frame have been estimated to be the order of 20 μm.

Preliminary results from data indicate that the tracker is aligned to the predicted mechanical precision.

7 Noise Studies

The spatial resolution and the hit finding efficiency depend on the strip pitch and on the signal–to–noise ratio.

To estimate the expected signal–to–noise ratio we use the mathematical model described in [9]. The total noise of a typical ladder, ENC_{ladder}, is obtained by adding the sources of noise in quadrature

$$\mathrm{ENC}_{ladder} = \mathrm{ENC}_{VA1} \oplus \mathrm{ENC}_{leak} \oplus \mathrm{ENC}_{res} \oplus \mathrm{ENC}_{ms}, \tag{1}$$

where ENC_{VA1} is the noise from the readout chip, ENC_{leak} is the noise from the leakage current, ENC_{res} is the noise from the biasing resistors and ENC_{ms} is the noise from the resistance of the metal traces. The parametrization for ENC_{VA1} was measured in [9]:

$$\mathrm{ENC}_{VA1} = 169e^- + 5.6\mathrm{e}^-\mathrm{C}_t/\mathrm{pF}, \tag{2}$$

where C_t is given in units of picofarads. In our model we assume that a minimum ionizing particle creates 25,000 electron–hole pairs when traversing $\simeq 300$ μm of silicon. The parameters contributing to the noise of a ladder have been measured in [9] and are listed in Table 1.

The calculated value for the strip resistance takes into account the reduction in the equivalent series resistance as explained in [13]. The total parallel resistance (R_p) is obtained by:

$$\frac{1}{R_p} = \frac{N}{R_{pol}} + \frac{1}{R_f}, \tag{3}$$

where N is the number of detectors in a ladder, R_{pol} is the dynamical resistance of the FOXFET for each detector and R_f is the feedback resistor of the preamplifier[5].

7.1 NOMAD–STAR

The sources of noise versus the length of a ladder are shown in Fig. 12. The dominant noise contribution comes from the metal strip resistance (ENC_{ms}), a characteristic inherent to long ladders for which the present detector design has not been optimized.

[5]It is expected to be at least 50 MΩ [10]; in our calculations we assumed $R_f = 100$ MΩ.

Parameter	Measured value for a detector	Calculated value for a ladder in NOMAD STAR	Calculated value for a ladder in the hybrid detector
Interstrip capacitance	1.2 pF/cm	86.4 pF	21.6 pF
Backplane capacitance	0.15 pF/cm	10.8 pF	2.7 pF
Total capacitance (C_t)	1.35 pF/cm	97.2 pF	24.3 pF
Strip resistance (R_{ms})	31.5 Ω/cm	756 Ω	189 Ω
Leakage current per strip (I_{leak})	0.04 nA	-	0.12 nA
Leakage current per strip (I_{leak})	0.08 nA	0.96 nA	-
FOXFET dynamical resistance	500 MΩ	-	-
Total parallel resistance (R_p)	-	29.4 MΩ	62.5 MΩ

Table 1: Summary of the parameters used in the model.

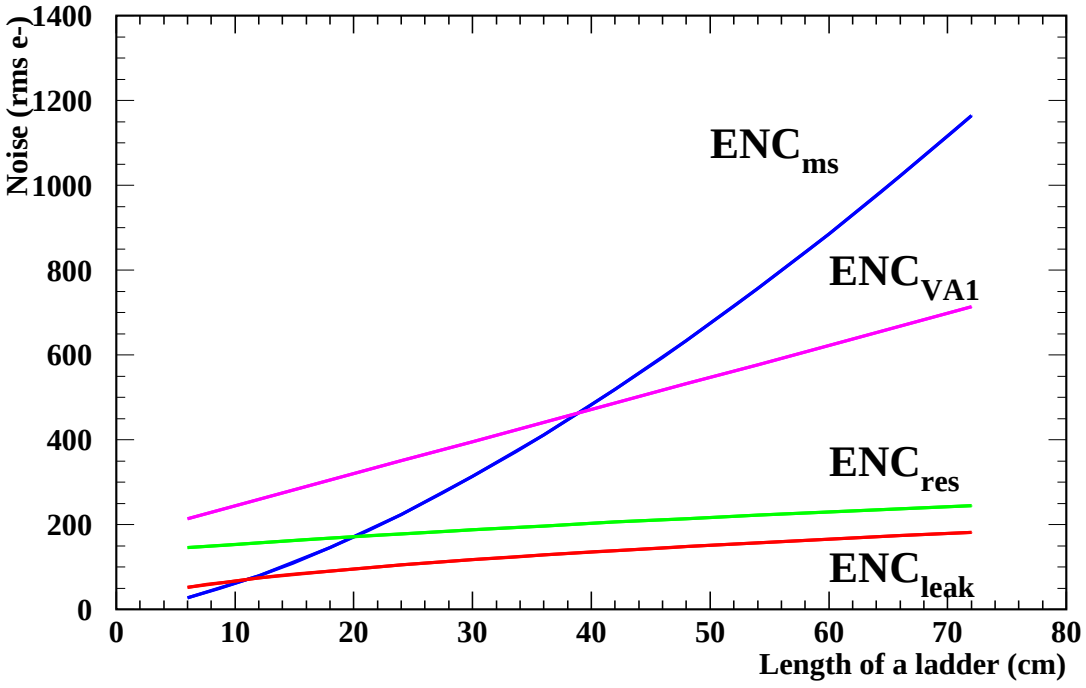

Figure 12: Sources of noise versus the length of a NOMAD–STAR ladder from theoretical predictions.

Prototype ladders were built in several steps and the signal–to–noise ratio was measured when ladders consisted of 1, 2, 3, 4, 9, 10, 11 and 12 detectors (a detector has a length of 6 cm). The solid curve in Fig. 13 shows the expected

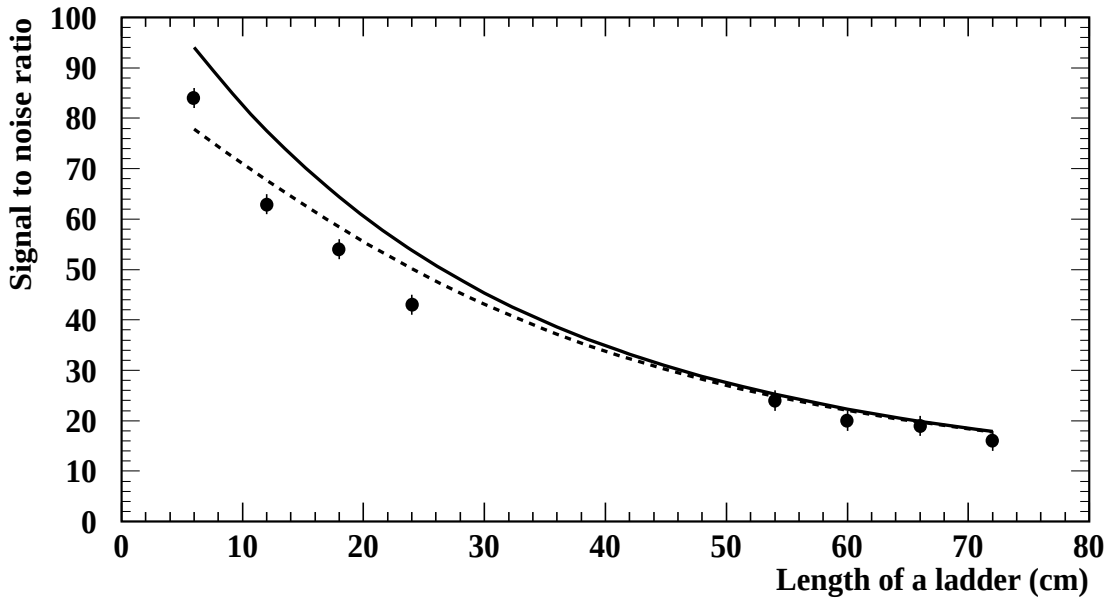

Figure 13: Calculated signal–to–noise ratio (solid curve) versus the length of a NOMAD–STAR ladder. The laboratory measurements are represented by the closed circles. The dashed curve corresponds to the calculated signal–to–noise ratio assuming an additional noise contribution from the hybrid (see text).

signal–to–noise ratio for a ladder as a function of its length. The laboratory measurements are represented by the closed circles. The disagreement between the calculated curve and the experimental data can be explained by an additional source of noise due to the hybrid printed circuit board. This additional source of noise is estimated to be of the order of 180 *rms* electrons. The dashed curve shows the expected behavior when this noise is added in quadrature to that of equation (2).

7.2 Hybrid Detector

Figure 14 shows the sources of noise versus the length of a ladder. As expected for short ladders, the dominant noise contribution comes from the load capacitance at the input of the amplifier (ENC_{VA1}). Predictions of the model and measurements performed using the radioactive source were compared. The signal–to–noise ratio was measured for a ladder with 1, 2 and 3 detectors (a detector has a length

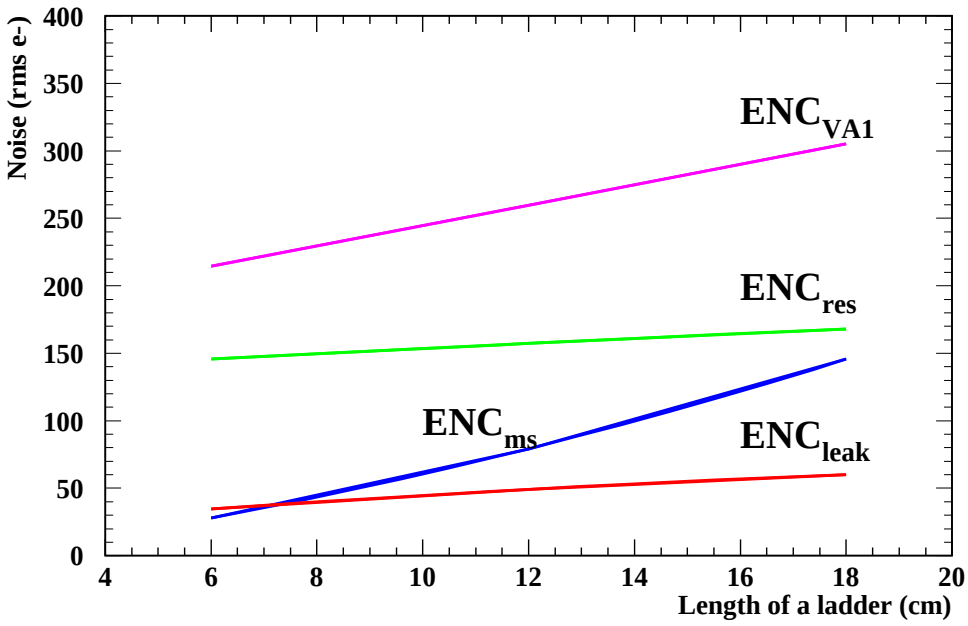

Figure 14: Sources of noise versus the length of a ladder of the hybrid detector from theoretical predictions.

of 6 cm), respectively. The results are displayed in Fig. 15, where laboratory measurements are represented by the closed circles. The solid curve shows the calculated signal–to–noise ratio for a ladder versus its length which is in a good agreement with the data. For completeness, we display in Fig. 15 the measured data from [9] with the old design of the hybrid printed circuit board (open circles). The improved design of the electronics results in a reduction of the total noise.

8 Results

8.1 A neutrino interaction in NOMAD–STAR

An example of a reconstructed ν_μ charged current interaction occurring in the target is depicted in Fig. 16.

8.2 Intrinsic resolution for the silicon detectors

A ladder of 9 detectors was tested in a particle beam at the CERN SPS [9]. The beam consisted of negative pions with momentum above 100 GeV/c, thus the multiple scattering was considered negligible. The ladder under test was mounted at one end of a telescope.

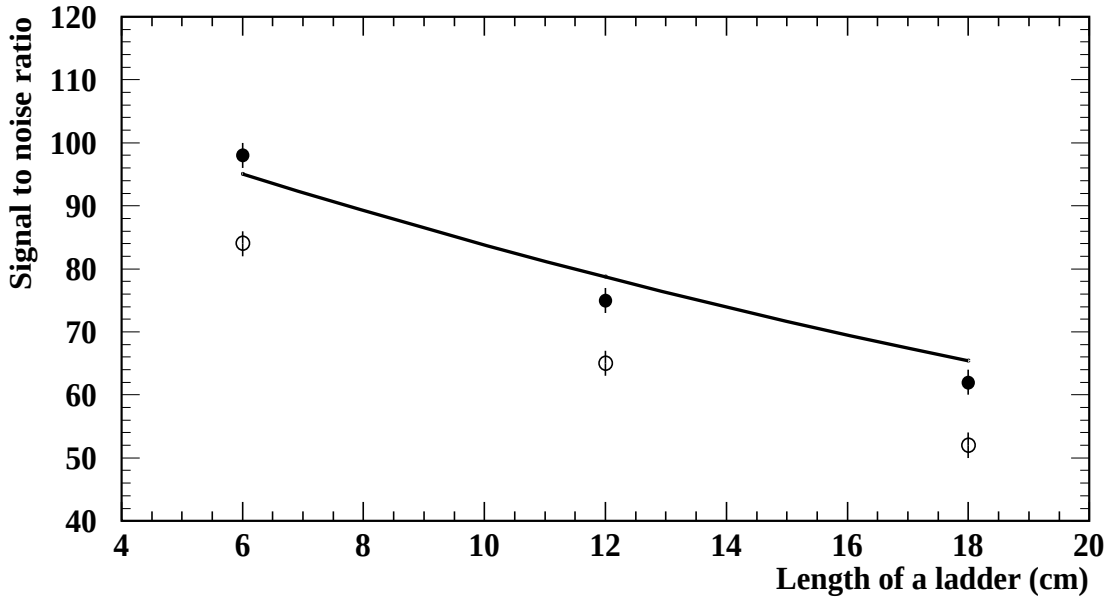

Figure 15: Calculated signal–to–noise ratio (solid curve) versus the length of the ladder of the hybrid detector. The laboratory measurements with the new (old) hybrid design are represented by the closed circles (open).

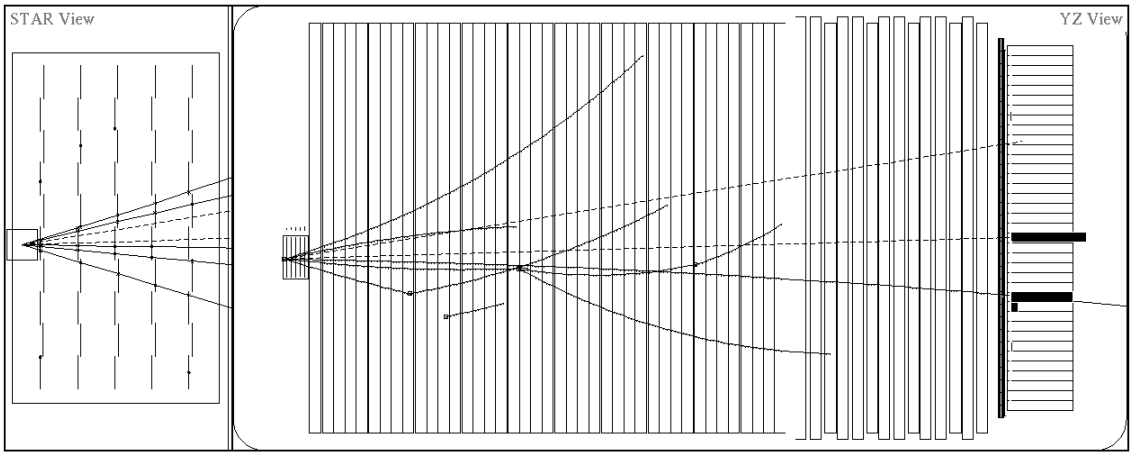

Figure 16: Reconstructed ν_μ charged current interaction inside the B_4C–silicon target (an expanded view of the target is shown on the left).

The intrinsic resolution was extracted from the distribution of residuals. A residual is defined as the difference between the impact point obtained from the charge collected on the detector strips and the point at which the extrapolated track reconstructed by the telescope intersects the plane of the detector. The distribution for residuals is displayed in Fig. 17 in which a 4.5 (2.5)σ cut–off value for the signal–to–noise ratio was applied for the central (adjacent) strips in a cluster.

The intrinsic spatial resolution of 6.0 μm was obtained by subtracting in quadrature the extrapolation errors (2.8 μm) from the residuals (6.6 μm). This resolution is sufficient for the determination of the impact parameter which is expected to be the order of 100 μm (see section 8.3).

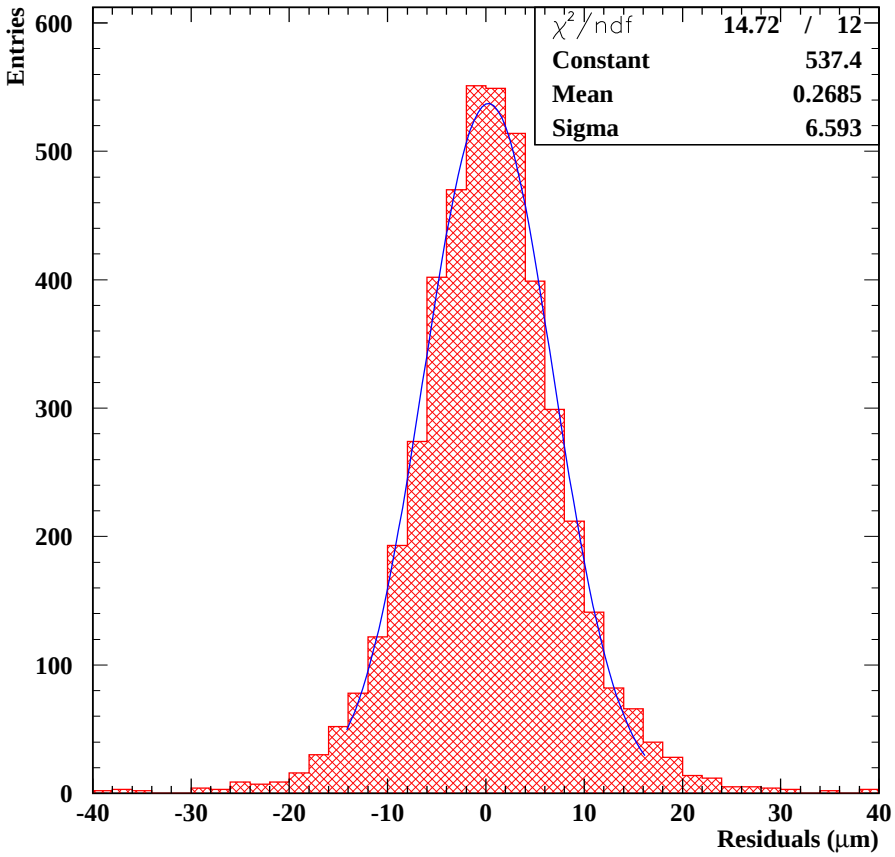

Figure 17: Residuals from a NOMAD-STAR ladder in a test beam.

8.3 Impact parameter in NOMAD–STAR

Figure 18a and b show an schematic drawing of the impact parameter for ν_τ and ν_μ charged current events, respectively.

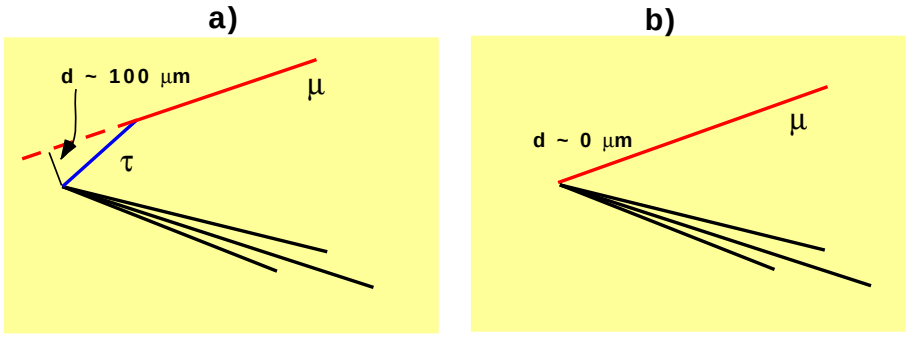

Figure 18: Schematic drawing for the impact parameter in a) ν_τ charged current and b) ν_μ charged current events.

The impact parameter (d) of a track is defined as the signed distance to the interaction vertex in the plane transverse to the beam direction. At SPS energies, the τ decay length corresponds to $\simeq$ 1.5 mm. The lifetime of the τ implies an impact parameter distribution that follows an exponential decay with characteristic length $c\tau$ = 88.6 μm [14]. For ν_μ charged current events (background) this distribution is roughly gaussian (resolution effects) and centered around zero. Its non–gaussian tails are due to multiple scattering.

The optimal way to disentangle ν_μ from ν_τ charged current events is to use the significance (s) of the impact parameter (d) defined as:

$$s = \frac{d}{\sigma_d}, \tag{4}$$

where σ_d is the error on the impact parameter which depends on the determination of the vertex and the parameters of the candidate track. The distribution of the significance has a zero mean and a width close to one for background events. Its width reflects resolution and multiple scattering effects. The significance is expected to be wider for ν_τ than for ν_μ charged current events.

Fig. 19a shows a preliminary impact parameter distribution for a muon in a sample of ν_μ charged current candidates in the 1997 data. In Fig 19b the corresponding impact parameter significance is also shown. These results are very encouraging. The origin of the events in the tail is currently being investigated.

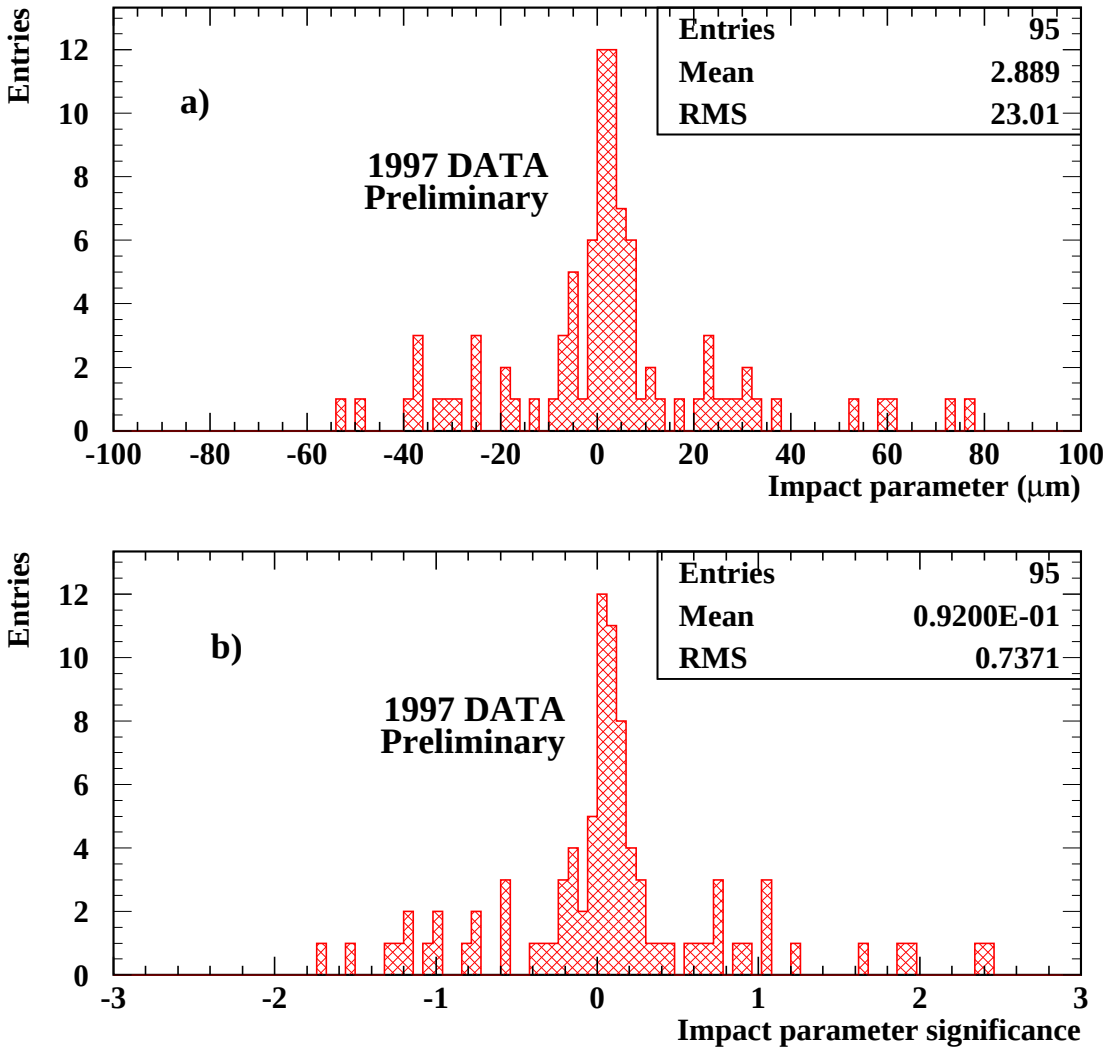

Figure 19: Preliminary results from 1997 data for a muon in a sample of ν_μ charged current candidates a) the impact parameter, b) the impact parameter significance (d/σ_d).

9 Conclusions

We have built two silicon trackers to investigate the possibility of using silicon detectors in future neutrino oscillations experiments. From NOMAD–STAR we have proven that long ladders of silicon detectors (72 cm) can be built, read out at one end only and have acceptable signal–to–noise ratio. The construction of the hybrid detector benefited from the experience acquired with NOMAD–STAR. We have improved both mechanical and electronic designs resulting in better signal–to–noise ratio, lower leakage current and smaller number of defective channels per ladder. These improvements have also reduced the steps needed during ladder construction and facilitated ladder debugging, which are essential for large scale experiments. Furthermore we have successfully described the sources of noise in both detectors with our proposed model. We have also shown that we can build a reliable surveying machine and perform a mechanical survey of the ladders to a few microns.

Using a test beam we have measured the intrinsic resolution in silicon with the expected accuracy ($<10\mu$m). We have also presented preliminary studies on the impact parameter distributions in NOMAD–STAR. Improvements on the results are expected since NOMAD–STAR continues to take data during the 1998 run and the analysis of the hybrid detector data is in progress.

Both detectors provide invaluable experience towards the construction of a large scale silicon tracker for future neutrino oscillation experiments.

Acknowledgements

We are indebted to the OPAL and CMS groups for providing support including the laboratory infrastructure. Special thanks to those of the NOMAD and TOSCA institutions who have provided funding and technical personnel for the two silicon projects.

References

[1] CHORUS Collaboration, E. Eskut *et al.*, Nucl. Inst. and Meth. **A401** (1997) 7-44.

[2] NOMAD Collaboration, J. Altegoer *et al.*, Nucl. Inst. and Meth. **A404** (1998) 96.

[3] J.J. Gomez-Cadenas, J.A. Hernando and A. Bueno, Nucl. Instr. and Meth. **A378** (1996) 196.

[4] J.J. Gomez-Cadenas and J.A. Hernando, Nucl. Instr. and Meth. **A381** (1996) 223-235.

[5] A. Ereditato, P. Strolin and G. Romano, *Study of a new experiment for the search of muon neutrino and tau neutrino oscillations*, CERN-PPE-96-106, June 1996; Nucl. Phys. Proc. Suppl. **54B** (1997) 139-150.

[6] A.S. Ayan *et al.*, *A high sensitivity short baseline experiment to search for* $\nu_\mu \leftrightarrow \nu_\tau$ *oscillation*, CERN-SPSC/97-5, SPSC/I213, March , 1997.

[7] J.J. Gomez-Cadenas, *Towards a Next Generation* $\nu_\mu(\nu_e) \leftrightarrow \nu_\tau$ *Oscillation Search Experiment*, Proceedings of the Faro Workshop, Faro, Portugal, September 1996. To be published by World. Sci. eds.

[8] G. Barichello *et al.*, *A* B_4C*–Silicon Target for the Detection of Neutrino Interactions* CERN-EP-98-21, 9 February 1998. Submitted to Nucl. Inst. and Meth.

[9] G. Barichello *et al.*, *Performance of Long Modules of Silicon Microstrip Detectors*, CERN-PPE 97-162, 11 December 1997. Submitted to Nucl. Inst. and Meth.

[10] O. Toker *et al.*, Nucl. Instr. and Meth. **A 340** (1994) 572.

[11] A. Zalewska, *The Silicon Tracker in the DELPHI Experiment at LEP2*, EPS–HEP Conference, Pa 17, Jerusalem, 19–26 August, 1997.

[12] P.P. Allport *etal*, Nucl. Inst. and Meth. **A 310** (1991) 155.

[13] I. Kipnis, *Noise analysis due to Strip Resistance in the ATLAS SCT Silicon Strip Module*, LBL Internal Report, LBNL-39307, August 1996.

[14] R.M. Barnett et al., Physical Review D54, 1 (1996) and 1997 off-year partial update for the 1998 edition available on the PDG WWW pages (URL: http://pdg.lbl.gov/).